Noname manuscript No.
(will be inserted by the editor)

The Pointing System of the *Herschel*⋆ Space Observatory

Description, Calibration, Performance and Improvements

Miguel Sánchez-Portal · Anthony Marston · Bruno Altieri · Hervé Aussel · Helmut Feuchtgruber · Ulrich Klaas · Hendrik Linz · Dieter Lutz · Bruno Merín · Thomas Müller · Markus Nielbock · Marc Oort · Göran Pilbratt · Micha Schmidt · Craig Stephenson · Mark Tuttlebee · The Herschel Pointing Working Group

Received: date / Accepted: date

⋆ Herschel is an ESA space observatory with science instruments provided by European-led Principal Investigator consortia and with important participation from NASA.

Miguel Sánchez-Portal
ISDEFE for ESA, Herschel Science Centre, European Space Astronomy Centre (ESAC), Villanueva de la Cañada, E-28691 Madrid, Spain
Tel.: +34-91-8131349 E-mail: miguel.sanchez@sciops.esa.int

Anthony Marston · Bruno Altieri · Bruno Merín
Herschel Science Centre, ESAC/ESA, Villanueva de la Cañada, E-28691 Madrid, Spain

Hervé Aussel
CNRS/Service d'Astrophysique, Bat. 709, 91191 Gif-sur-Yvette, France

Helmut Feuchtgruber · Dieter Lutz · Thomas Müller
Max-Planck-Institut für extraterrestrische Physik, Postfach 1312, 85741 Garching, Germany

Ulrich Klaas · Hendrik Linz · Markus Nielbock
Max-Planck-Institut für Astronomie, Königstuhl 17, D-69117 Heidelberg, Germany

Marc Oort
Dutch Space B.V., Leiden, The Netherlands.

Göran Pilbratt
ESA Astrophysics Missions Div./Research and Scientific Support Dept., ESTEC/SRE-SA, Keplerlaan 1, NL-2201 AZ Noordwijk, The Netherlands

Micha Schmidt
European Space Operations Centre (ESOC)/ESA, Robert-Bosch Strasse 5, D-64293 Darmstadt, Germany

Craig Stephenson
Telespazio Vega for ESA, Herschel Science Centre, ESAC, Villanueva de la Cañada, E-28691 Madrid, Spain

arXiv:1405.3186v1 [astro-ph.IM] 13 May 2014

Abstract We present the activities carried out to calibrate and characterise the performance of the elements of attitude control and measurement on board the Herschel spacecraft. The main calibration parameters and the evolution of the indicators of the pointing performance are described, from the initial values derived from the observations carried out in the performance verification phase to those attained in the last year and half of mission, an absolute pointing error around or even below 1 arcsec, a spatial relative pointing error of some 1 arcsec and a pointing stability below 0.2 arsec. The actions carried out at the ground segment to improve the spacecraft pointing measurements are outlined. On-going and future developments towards a final refinement of the Herschel astrometry are also summarised. A brief description of the different components of the attitude control and measurement system (both in the space and in the ground segments) is also given for reference. We stress the importance of the cooperation between the different actors (scientists, flight dynamics and systems engineers, attitude control and measurement hardware designers, star-tracker manufacturers, etc.) to attain the final level of performance.

Keywords Herschel Space Observatory · spacecraft · pointing · alignment · calibration · performance

1 Introduction

The Herschel Space Observatory [22] is the fourth "cornerstone" mission in the ESA Horizon 2000 science programme. It has been the first large aperture space far–infrared (FIR)/sub–mm observatory, performing photometry and spectroscopy in the 55–672 μm wavelength range. The observatory consisted of a telescope with a large (3.5 m) monolithic low emissivity passively cooled mirror and three focal plane science instruments enclosed in a large HeII cryostat: The PACS instrument [23], consisting of *(a)* a dual-band photometer, comprising a "blue photometer" with two filters mounted in a wheel, allowing to select a range centred at either 70 μm or 100 μm and a "red photometer" covering a spectral range centred at 160 μm; and *(b)* an integral field spectrometer in the range 57-210 μm. The photometric bands covered the same field-of-view (FoV), while the FoV of the spectrometer was offset from the photometer. The SPIRE instrument [13] consisted of a three-band imaging photometer and an imaging Fourier Transform Spectrometer. As for the PACS instrument, the photometer and spectrometer did not operate simultaneously. The three photometer arrays provided broad-band photometry in bands centred at 250, 350 and 500 μm with a common FoV, and the spectrometer was also offset from the photometer. Finally, the HIFI instrument [7] was a high-resolution heterodyne spectrometer with a continuous coverage from 480 to 1250 GHz in five bands, plus two bands providing a coverage of

Mark Tuttlebee
SCISYS for ESA, ESOC, Robert-Bosch Strasse 5, D-64293 Darmstadt, Germany

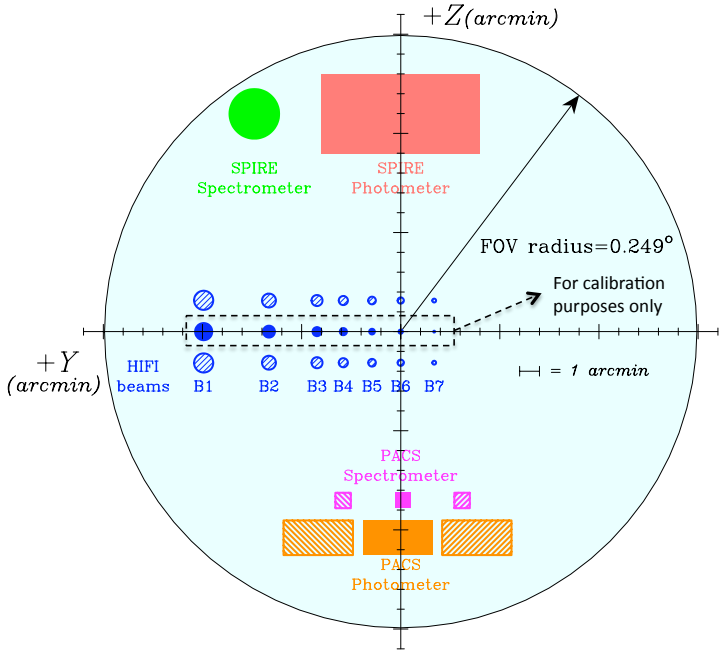

Fig. 1 Location of the different instruments' apertures within the Herschel FoV

the 1410–1910 GHz range. Both polarisations of the astronomical signal were detected for maximum sensitivity. To cover a wide frequency range with high sensitivity, HIFI was designed to have 7 mixer bands and 14 Local Oscillator sub-bands (two frequency sections per band). Figure 1 shows the position of the instruments' apertures within the Herschel FoV.

The Herschel spacecraft (S/C) had a modular design, comprising the Extended Payload Module (EPLM) and the Service Module (SVM). The EPLM consisted of the payload module described above, the sunshade and solar array and payload associated equipment. The SVM housed "warm" payload electronics and provided services such as power, attitude and orbit control, the on-board data handling and command execution, communications, and safety.

The Herschel S/C was stabilised in three-axes. The attitude was commanded by means of reaction wheels and controlled using star trackers and gyroscopes, as described in Section 2. The S/C pointing modes were based either on stare pointings (fine pointing mode) or moving pointings at constant rate (line scan mode). Raster maps are "grids" of stare pointings at regular spacings; scan maps are sequences of line scans at regular spacing. Allowed scan angular speed ranged from 0.1 arcsec/s to 1 arcmin/s. In addition, the Herschel spacecraft could track moving Solar System targets at rates up to 10 arcsec/min. The S/C slewed between different pointing positions at rates up to 7 arcmin/s.

The pointing calibration tasks were aimed, on the one hand, to provide an accurate alignment of the different fields of view of each instrument and instrument mode described above with respect to the telescope and the S/C attitude reference frame, and on the other, to characterise the performance of the various pointing modes. This paper describes these activities and is structured as follows: in Section 2, we discuss the basic elements of the Attitude Control and Measurement System (ACMS) and the route of telemetry (TM) data from the spacecraft to the Herschel Science Centre (HSC) at the European Space Astronomy Centre (ESAC). Section 3 is devoted to the pointing-related products generated at the HSC: the pointing product, the ACMS TM product and the Spacecraft/Instrument Alignment Matrices (SIAM) product. Section 4 deals with the main calibration parameters of the Herschel spacecraft pointing system and historical description of the evolution of the indicators of its performance, that in general met or surpassed the requirements set. However, given a clear scientific motivation for further improvement (see Section 4), an outstanding effort has been done and is still being invested: in Section 5, the work carried out within the ground segment centres to improve the S/C pointing measurements is described. On-going and future developments towards a final refinement of the Herschel astrometry are also described.

2 Basic elements and operation of the ACMS

The control of the positioning of the Herschel spacecraft (S/C) was carried out by its Attitude Control and Measurement System (ACMS). The main components were [1]: *(i)* the attitude control computer (ACC); *(ii)* gyroscopes (GYR; four units); *(iii)* star trackers (STR): two units, with boresights approximately opposite to that of the telescope; *(iv)* the assembly of four reaction wheels (RWA) to perform pointing manoeuvres; *(v)* the Reaction control system (RCS), i.e. the set of thrusters used for orbit manoeuvres and reaction wheel biasing; *(vi)* the sun acquisition sensors (SAS); *(vii)* the coarse rate sensors (CRS); and *(viii)* the attitude anomaly detectors (AAD). The different elements of the ACMS are depicted in Fig. 2 and described in [1].

The star trackers (STR) were small telescopes with CCD detectors whose main function was the determination of the S/C attitude. The Herschel S/C had two (cold) redundant autonomous units built by Selex Galileo S.p.A. [2]. The STR telescope had a focal length of 30 mm and an f/number of 1.2, yielding a large FoV of $16.4 \times 16.4\,\mathrm{deg}^2$. The CCD detector used was the Atmel TH78900, with 512×512 pixels of $17\,\mu$m. The plate scale was therefore 116.9 arcsec/pixel (the CCD area is slightly larger than the FoV). The Herschel STRs had the ability to determine the inertial position from a "lost in space" situation, or tracking from a known attitude. To this end, an on-board star catalogue, based on Hipparcos, was used. The criteria applied to build this catalogue included a specific range of brightness, a B–V colour threshold, a low variability tolerance, reduced proper motion and absence of close companions or neighbours [6]. The on-board catalogue contained 3599 stars,

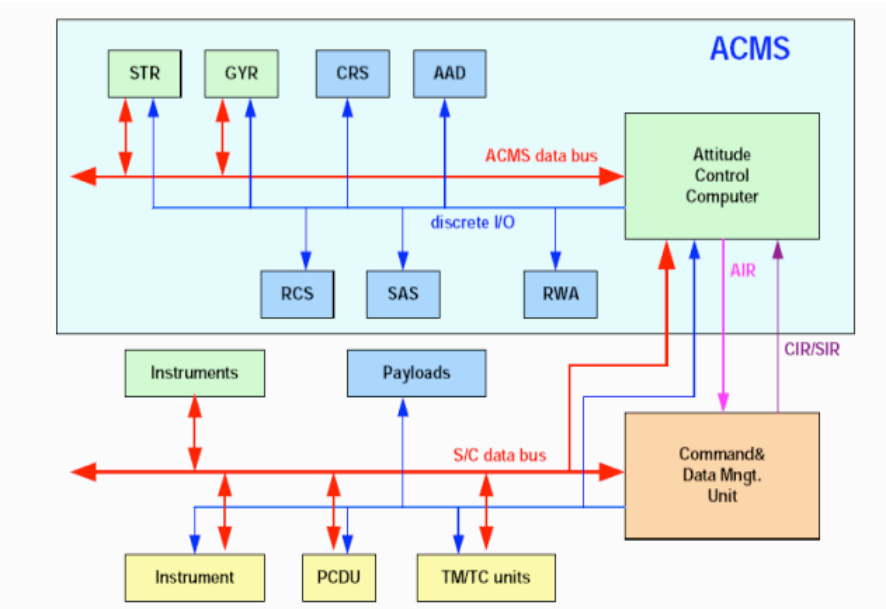

Fig. 2 ACMS block diagram (reproduced from [17]). The individual elements depicted and their acronyms are described in the text.

out of which originally 3047 (85%, but cf. Section 4.5) were enabled for tracking purposes. A minimum of 3 stars should be acquired within the FoV. Due to hardware limitations, a maximum of 9 stars could be simultaneously used for attitude determination. Nevertheless, there was an enhanced performance mode called "interlacing function", only applicable if ≥ 15 trackable stars were located within the FoV. In this mode, the STR determined the attitude using two different sets of stars from two consecutive frames, (i.e. each set of stars were sampled at half the nominal 4 Hz sampling frequency). In this way, up to 18 stars could be used for attitude determination. Due to the large weight of the STR measures in the attitude estimation, the highly undersampled STR FoV was the largest contributor to the absolute pointing error (APE). On top of that, the position-dependent STR bias was caused by flat-fielding effects and optical distortions. On average, the contribution to the APE was $0.8 \times \sqrt{2}$ arcsec.

The mounting of the STRs with respect to the S/C and telescope viewing direction is shown in Fig. 3 (left). Note that the STRs pointed approximately at 180° w.r.t. the telescope boresight ($+X_{SCA}$; see definition in Section 3 below). Both STRs were mounted on a carbon fibre platform suspended by struts from the lower dome of the cryostat vacuum vessel (CVV) as shown in Fig. 3 (right). The struts were partly made of glass fibre, to minimise the conducted heat input to the CVV, and partly of carbon fibre, to minimise the thermoelastic distortions [9].

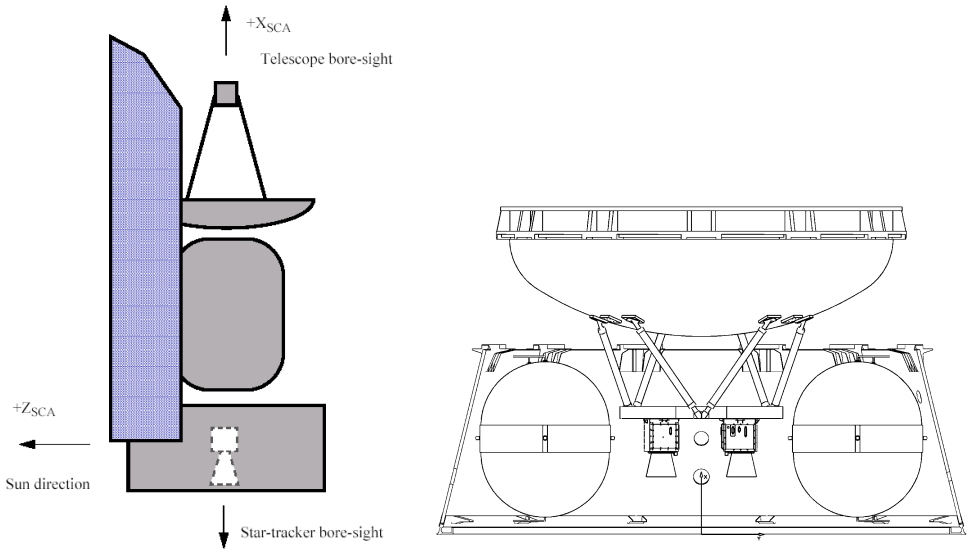

Fig. 3 Left: Herschel spacecraft axes, telescope and boresight of the STRs (reproduced from [17]). Right: diagram of the two redundant STR mountings below the CVV. The STRs are shown as the two identical, small square boxes with conical baffles (reproduced from [9])

Only one STR could be operative at a given time, the other unit kept as backup. The possibility of using both STRs simultaneously to ease the calibration of their mutual misalignment was ruled out due to the alteration of the pointing due thermoelastic distortion caused by the excessive heat dissipated.

The Herschel S/C used hemispherical resonating gyroscopes. These consist of a thin-walled quartz shell that is energized by an electrical field to produce a vibration pattern within itself. The gyroscopes were used to sense and respond to changes in the inertial orientation of its spin axis. Rate/rate-integrating gyroscopes provided high-precision measures of the S/C angular speed. The Herschel's ACMS was provided with four gyroscopes mounted in a tetrahedral configuration. The four gyroscopes were hot-redundant. The fourth gyroscope was not used for control, but served to detect an inconsistency in the output of the other three.

Estimates of the satellite attitude quaternion[1] and inertial rate vector were obtained combining data from GYR and STR. The estimator was based on a "model replacement approach" in which a dynamical model for the evolution of the quaternion states was replaced by integration of the kinematics equations of motion, driven by angular rate measurements from the gyro. In the nominal estimator the state (attitude quaternion, rate estimate and GYR

[1] Quaternions are a single example of a more general class of hypercomplex numbers. By analogy with the complex numbers, a quaternion can also be written as a linear combination of a real and three imaginary components. It is easy to represent the concatenation of rotations in quaternion format, constituting a very convenient and compact means of representing S/C attitudes. It is outside the scope of this paper to give even an introduction to quaternions. A good introduction to this topic is given in [28].

bias) was propagated from the previous estimate using the gyro data. This was then combined with the latest STR measurement to obtain an updated state estimate which was subsequently used for control. The main reason for the inclusion of GYR data in the model is that the STR measurements were delayed by 1.5 cycles due to integration and internal processing. Finally, the actuation was performed by means of the RWA.

The attitude information derived by the ACMS was down-linked at a rate of 4 Hz[2] when the S/C is in normal science mode (SCM) operation. The telemetry (TM) was processed at the Mission Operations Centre (MOC). The Flight Dynamics Team produced the so-called "attitude history file" (AHF) per operations day (OD) basis. The AHF packed the ACMS SCM TM generated at 4 Hz for slew, point and line scan operations. It was an ASCII-formatted file that included the on-board time, commanded attitude, ACMS-processed attitude (the so-called filtered attitude), three-axes X, Y and Z calibrated angular rates, S/C solar aspect angle (SAA), measurement quality flags etc. The AHF was transferred automatically to the HSC within 8 hours of the end of the OD. It triggered the start of the processing of auxiliary products (e.g. housekeeping telemetry, radiation monitory data, orbit data, etc.) at the HSC.

3 Pointing products created at the HSC

The information produced by the ACMS was processed (and is still re-processed) by the HSC and stored in "products". These data structures can be accessed from the observation context (a sort of container of the scientific and housekeeping data belonging to a given observation). The pointing-related products belong to the "auxiliary products" category. Three classes have been defined: pointing product, ACMS TM product and spacecraft/instrument alignment matrices' (SIAM) product.

The pointing product is the most important of these data structures. It packs the information contained in the AHF, combined with up-link information from the planned observation sequence (POS) file. The pointing product consists of sequences of table data sets (analogous to FITS binary tables) including: on-board time, commanded attitude quaternion, different estimates of the attained attitude quaternion, attitude error estimates, number of tracked stars, etc. It is produced per OD, but sliced per observation. The detailed contents of the product can be found in Table 11.

The ACMS TM product contains all the relevant information required to re-estimate the S/C attitude from scratch. Sliced per observation, uses essential TM, SCM TM and diagnostics TM. It includes many ACMS database parameters as metadata entries (analogous to the FITS header's keywords). Product's data records include estimated attitude quaternion, STR quaternion, calibrated gyro rates, IDs, positions, magnitudes and colours of tracked stars, GYR calibration parameters etc.

[2] The actual packet rate was 1 Hz but many ACMS parameters were super-commutated (four samples per packet).

The spacecraft/instrument alignment matrices (SIAM) product contains 3×3 proper orthogonal rotation matrices $\mathrm{DCM}_{INS-ACA}$ converting the coordinates of a vector in the Herschel spacecraft reference frame (spacecraft control axes, SCA; also known as attitude control axes, ACA) into a given instrument reference frame (INS), i.e.:

$$\begin{aligned} \mathbf{u}_{INS} &= DCM_{INS-SCA} \cdot \mathbf{u}_{SCA} \\ \mathbf{u}_{SCA} &= DCM^{T}_{INS-SCA} \cdot \mathbf{u}_{INS} \end{aligned} \tag{1}$$

The product contains one rotation matrix per instrument (see a brief description of the instruments in Section in 1), i.e. 2 matrices for PACS (one for the photometer aperture and one for the spectrometer one), 56 matrices for HIFI (the apertures are defined for the 7 bands, 2 sub-bands per band, 2 polarisations and 2 chopper positions) and 75 matrices for SPIRE (the SPIRE apertures are defined at pixel level, 17 for the photometer and 57 for the spectrometer, plus an additional aperture for the so-called SPIRE/PACS parallel mode; this aperture is placed in the midpoint between the PACS and SPIRE photometers, approximately in the centre of the telescope FoV. In normal scientific operation, only the central photometer and spectrometer apertures, plus the parallel mode one, are used). The alignment matrices were determined by means of dedicated calibration observations, mainly during performance verification phase (see Section 4). For astrometrical purposes, there are two valid SIAM files across the whole mission: 0122_0001 ($\mathrm{OD} < 320$) and 0341_0001($\mathrm{OD} \geq 320$). This is due to the change in the STR CCD reference temperature that took place in OD320 and will be thoroughly explained in the next section.

4 Main pointing calibration parameters and evolution of the pointing performance

The main pointing calibration activities were carried out during commissioning (CoP; some 60 ODs) and performance verification (PVP; approximately 90 ODs) phases using the scientific instruments. These calibrations were aimed, on the one hand, to accurately determine the location of the different instrument apertures (i.e. computation of the SIAMs), and on the other hand, to derive the main figures of merit characterising the pointing performance. These are according to [8] the Absolute Pointing Error (APE), defined as the angular separation between the desired direction and the instantaneous actual direction; the Pointing Drift Error (PDE), defined as the angular separation between the average pointing direction over some interval (nominally 55 min) and a similar average at a later time (nominally after 24 hours), is a measure of the long-term stability of the S/C pointing, while the Relative Pointing Error (RPE, also referred to as pointing stability) is the angular separation between the instantaneous pointing direction and the short-time average pointing direction at a given time period (fixed at 60 s); finally, the Spatial Relative

Pointing Error (SRPE) is defined as the angular separation between the average orientation of the satellite fixed axis and a pointing reference axis which is defined relative to an initial reference direction: this measurement is important to characterise the accuracy of the relative astrometry in a map comprising several pointings (e.g. a raster or scan map).

The pointing error specifications are expressed as half-cone angles of the line-of-sight (LoS) and half-sector angles around the LoS. They are specified at a temporal probability level of 68%, which implies that the error will be less than the requirement for 68% of the time for each pointing direction. For Herschel, it was required that the APE in stare pointings was 3.7 arcsec (LoS) and 3.0 arcmin (around LoS). The PDE requirement (measured within a 24 h period) is 1.20 arcsec (LoS) and 3.0 arcmin (around LoS). The RPE requirement (for a period of 60 s) is 0.30 arcsec (LoS) and 1.5 arcmin (around LoS). Finally, regarding the spatial relative pointing accuracy, it was required that, in consecutive pointings within a $4^\circ \times 4^\circ$ spherical area, the SRPE of all pointings following the initial pointing, as referred to the average pointing direction of the first pointing shall be less than 1 arcsec (LoS). Table 1 summarises the initial requirements for the main pointing figures of merit as given in the early mission definition phase and their predicted performance from pre-launch testing campaigns. It was anticipated a non-compliance of the SRPE (2.24 arcsec predicted vs. 1.0 arcsec required) but the rest of the requirements were clearly met or exceeded. As will be shown below, the in-orbit performance of the Herschel S/C confirmed these predictions. However, beyond the early defined requirements shown in Table 1 (issued when the final characteristics of the instruments were only barely known), and given Herschel instruments' beams as small as 5 arcsec FWHM at the shortest wavelengths, there was a clear scientific motivation for further improvement, for better centring of spectroscopic observations on source, as well as for better a posteriori reconstruction of the actual pointing in imaging and spectroscopy.

Table 1 Initial requirements and pre-flight predicted performance of key pointing accuracy indicators. Goal conditions assume 18 stars available for guidance within the STR (i.e. the maximum possible number).

	Baseline (arcsec)		Goals (arcsec)	
Parameter	Requirement	Prediction	Requirement	Prediction
APE point	3.7	2.24	1.5	1.34
APE scan	3.7	2.36	1.5	1.42
SRPE	1.0	2.21	1.0	1.52
RPE	0.3	0.24	–	–
PDE	1.2	088	–	–

The SIAM matrices were initially defined by means of accurate measurements performed on-ground during the assembly, integration and verification phase (AIV). In flight, new SIAMs were derived by planning and executing dedicated calibration observations with the PACS, SPIRE and HIFI instru-

ments, as described in [17] and [25]. The first calibration (serving as reference for the initial bulk shift of all instruments' apertures with respect to the original SIAM set used at launch time), the alignment of the PACS photometer aperture, and almost all measurements of the pointing performance were carried out with the PACS photometer point-source mode and the "blue" camera with the 70 mum filter (the shortest photometric wavelength) since this configuration gave the best spatial resolution. A thorough description of the PACS chopped point-source photometry observing mode is given in [20]. A catalogue of several hundred stars with strong, purely photospheric FIR flux densities compiled by the PACS Instrument Control Centre (ICC) [19] was used, in order to ensure that their FIR emission was as compact as possible (i.e. no dust shells). The observations were processed using dedicated scripts within the Herschel Interactive Processing Environment (HIPE; [21]). The sky positions of the centroids of the target stars within the 70 μm PACS photometer maps, derived from the Herschel astrometry were compared with the catalogue positions (either Hipparcos or 2MASS). This was done for relatively large sets of targets (typically more than 40) in order to obtain distributions of offsets along the Y and Z axes. These were generally very well fitted by Gaussian distributions. The (Y, Z) average offsets were used to derive the alignment matrices, while the standard deviations of the distributions were used to derive a proxy, $\mathrm{APE}^{\dagger} \equiv \sqrt{\sigma_Y^2 + \sigma_Z^2}$, for the absolute pointing accuracy that would be achieved with the alignments corrected[3].

The original set of matrices obtained from PVP observations were derived with a STR CCD reference temperature of 20°C. In OD 320, the reference temperature was lowered to -10°C in order to reduce the number of "warm" STR CCD pixels (see below). As a result, a bulk shift of all instruments' apertures occurred and a new SIAM set was computed accordingly. This new collection of matrices was used throughout the rest of the S/C operations.

The main figures of merit, namely APE, SRPE and RPE were derived from PACS photometer PVP observations (see Section 4.1)[4]. The pointing drift dependency on the Solar Aspect Angle (SAA; angle from the S/C boresight X axis to the Sun vector) was also assessed (and estimated to be significant only for $\mathrm{SAA} \geq 110°$).

In Routine Science Phase (RSP), a new pointing calibration plan was designed [24]; its goal was twofold: on the one hand, to provide a periodic verification of the pointing calibration (alignment matrices), and on the other, to detect potential variations of the pointing performance. More than one-thousand pointing calibrations have been performed during RSP. The PACS Photometer in point-source mode (with dithering) and the "blue camera" with the 70 μm filter was preferentially used. But some scan map observations were

[3] Beware that $\mathrm{APE}^{\dagger}$ is not the proper APE, that is defined in temporal terms. A justification for the use of this proxy is given in [26], where it is shown that it introduces an additional error of typically only 0.1 arcsec.

[4] The PDE was not explicitly measured within PVP, but the long-stare pointing tests carried out indicated that the requirement was met, provided that the S/C was kept out of "warm" attitudes (see definition below).

included as well (PACS Photometer mini-map mode). The pointing performance was found to be similar to that obtained in point-source mode (see below). Also, an accurate calibration of the relative misalignment of the two STR units (prime and backup) was performed in OD732 (44 calibration observations were planned and executed with the backup STR unit configured as operational. In this way, not only the misalignment of both STRs but also the pointing accuracy achievable with the backup unit was estimated). Since the accessible area of the sky was restricted during the daily telecommunications period (DTCP), RSP pointing calibration observations compatible with the DTCP restriction were generally selected. This optimised the scientific return by not blocking with these calibration measurements observing time outside the DTCP with much more flexible pointing constraints (and therefore more suitable for general scientific observations). However, the drawback of this strategy was that position-dependent effects could not be detected at earlier stages (See Section 4.2 below).

One of the main pointing issues found early in the mission was the existence of the so-called "speed bumps", namely events of departure from the nominal attitude observed in scan maps, easily recognizable in the S/C velocity norm profile as local maxima ("bumps"). The cause of these anomalies was traced by the ACMS manufactures to the existence of a growing number of high-signal or "warm" pixels in the STR CCD. This problem was corrected by lowering the reference temperature of the STR CCD to -10°C in OD320. Unfortunately, a side effect of this action was an important increment of STR plate scale errors[5] (equivalent to unequal focal length corrections in the Y and Z axes), introduced by the STR CCD temperature change. These errors produced systematic, orientation-dependent offsets. The problem was partially corrected by applying a one-dimensional STR focal plane correction that took place in OD762 (this was implemented by modifying the nominal on-board focal length value of the STR, f_0. This is equivalent to assume identical focal length corrections in both axes, i.e. $\Delta f_Y = \Delta f_Z$). The final on-board performance was greatly improved thanks to three major developments, implemented step by step:

1. In a first step (tested in OD858 and used from OD866 to OD1010), a linear two-dimensional STR correction (i.e. $\Delta f_Y \neq \Delta f_Z$) was uploaded, boosting the pointing performance to APE$^{\dagger} \simeq 1.0$ – 1.1 arcsec.
2. In a second step (since OD1011), the full STR focal plane distortion correction (8 polynomial coefficients per axis), computed in parallel by the PACS ICC and the ESA/Flight Dynamics Systems (FDS) team at the MOC was uploaded, producing a further improvement in the performance, APE$^{\dagger} \simeq 0.8$ – 0.9 arcsec.
3. In a third step (since OD1032), several "dubious" stars (see Section 4.5) were removed from the on-board STR tracking catalogue, yielding the final

[5] Minor STR plate scale errors were present in the early phases of the mission. The result of the CCD reference temperature lowering was a substantial increase of the effect. The attitude measurements have been improved by applying corrections in the ground processing. See Table 10 and Section 5.1.

APE† figure rather homogenous in the sky, provided that enough tracking stars were available and that "cold" S/C attitude conditions applied[6].

In the following subsections, the evolution of the pointing performance is detailed.

4.1 Pointing performance from launch to OD320

The most representative APE† estimate was derived using PACS photometer point source observations during the PVP. A large set of observations (approximately 250) in six ODs (38, 64, 86, 92, 101 & 104) were used to derive the PACS photometer aperture position (named `P01_0`) and also the absolute pointing performance figure. In addition, a large pointing campaign was implemented in OD274 to determine the pointing performance depending on the STR interlacing (il; see Section 2) mode: *il-disabled*, up to 9 stars tracked at a time, and *il-enabled*, from 15 to 18 stars sampled alternatively in two "planes". The results are summarized in Table 2. The APE† was measured to be between 1.9 and 2.2 arcsec depending on the enabling of interlacing.

Table 2 APE† measurements (1^{st} period). $\langle \Delta Y \rangle$ and $\langle \Delta Z \rangle$ are the average offsets of the Y and Z positions of the centroids of the measured stars w.r.t. the origin of the PACS photometer coordinate frame [20]. These average offsets were used to compute the SIAM of the PACS photometer `P01_0` aperture and therefore not considered for pointing error computation purposes.

OD range	$\langle \Delta Y \rangle$ (arcsec)	$\langle \Delta Z \rangle$ (arcsec)	σ_Y (arcsec)	σ_Z (arcsec)	APE† (arcsec)
38–104 (250 meas.)	–	–	1.09	1.56	1.90
274 (all, 102 meas.)	-0.45	-1.71	1.23	1.51	1.94
274 (il-disab, 55 meas.)	-0.35	-1.67	1.23	1.72	2.24
274 (il-enab, 47 meas.)	-0.57	-1.75	0.93	1.22	1.53

4.2 Pointing performance from OD320 to OD762

As mentioned above, the event marking the onset of this long period is the lowering of the STR CCD reference temperature from 20 to -10°C that corrected the "speed bumps" problem at the price of increasing the STR plate scale errors that produced systematic but boresight-dependent offsets. Shortly after the STR CCD temperature adjustment (OD385) the first routine pointing calibration observations were executed. The plate scale errors translated

[6] The term "cold" refers to those S/C attitudes that keep the service module away from heating by solar radiation, in contrast to "warm" attitudes. Originally, only those with SAA $\geq 110°$ were considered as problematic due to the risk of heating some components of the STR support structure.

into variations of the dispersion of the distribution of pointing calibration observations; nevertheless, this was not clearly and immediately reflected in the statistical results obtained from the pointing calibration campaigns: while in cycles[7] 15–22, the APE† was consistent with PVP results, an outstanding increase was observed in cycles 23–31 and a decrease thereafter, as summarized in Table 3. The investigation revealed that the effect was very small when the distribution of tracked stars was uniform across the STR FoV, but large, sometimes as much as ~ 8 arcsec when the distribution of guide stars was asymmetric (see a detailed explanation in Sect. 2.4.2 of [27]. This explains the different behaviour of the dispersion of measurements depending on the considered period, since, as explained above, the RSP pointing calibration observations were preferentially performed in the relatively small sky area compatible with the DTCP constraints. This sky patch changes and moves slowly across the sky and therefore varies usually little within the time frame of a cycle. Thus, the configuration of guide stars for all pointing observations obtained within a cycle are generally similar.

Table 3 APE† measurements (2^{nd} period)

Cycles	OD range	No. observations	$\langle \Delta Y \rangle$ (arcsec)	$\langle \Delta Z \rangle$ (arcsec)	σ_Y (arcsec)	σ_Z (arcsec)	APE† (arcsec)
15–22	385–496	45	-0.83	-0.17	0.85	1.80	1.99
23–31	497–622	51	-0.58	-0.30	1.33	2.26	2.62
32–36	623–692	40	-0.08	0.19	1.05	2.03	2.28
33–36	637–692	34	-0.16	0.56	1.06	1.67	1.98
37–39	–	22	-0.01	-0.58	1.10	1.19	1.62
–	731	17	0.27	-0.57	1.12	2.05	2.33
–	733	21	-0.62	0.55	1.28	2.65	2.95

An average of a large subset of observations in cycles 15–40 was performed (comprising nearly 200 observations). The results are shown in Table 4. This is considered a representative value of the mean absolute accuracy achieved in this period. The largest outlier is at nearly 7 arcsec from the barycenter of the distribution, a value that is consistent with some extreme cases reported by observers. Incidentally, the plate scale errors affected mainly the prime STR (STR1), with a negligible effect in the backup unit (STR2) due to the initial detector position[8].

[7] A cycle is a series of ODs where all the instruments are used in sequence. Typically comprises 14 ODs.

[8] As demonstrated by measurements derived from CCD dumps performed at the initial and final STR2 CCD reference temperature.

Table 4 average APE† for periods 2^{nd} –4^{th} (see text for details)

Cycles	OD range	No. observations	$\langle \Delta Y \rangle$ (arcsec)	$\langle \Delta Z \rangle$ (arcsec)	σ_Y (arcsec)	σ_Z (arcsec)	APE† (arcsec)
2^{nd} period							
15–40	385–733	196	-0.40	-0.13	1.17	2.05	2.36
3^{rd} period							
–	764	42	-0.26	0.90	0.92	1.12	1.45
4^{th} period							
–	858	43	-0.27	0.54	0.70	0.65	0.95
49-51	872–900	36	-0.13	0.20	0.79	0.80	1.12

4.3 Pointing performance from OD762 to OD866 (STR1 1D correction)

As explained above, a first on-board corrective action was performed in OD762, by up-loading a new nominal on-board focal length value of the STR (See Section 2.3.1 of [27] for details on the determination of the correction applied). The pointing performance was revisited in OD764 (42 pointing calibration observations), with very positive results, as shown in Table 4.

4.4 Pointing performance from OD866 to OD1010 (STR1 2D correction)

The linear 2D correction (i.e. two separate, linear correction factors to the Y and Z axes; see Section 2.3.1 of [27] for details on the determination of the correction) is the main pointing improvement carried out during the S/C operation. It was tested in DTCP858. The first assessment done by FDS was very positive. The pointing performance was verified in OD858 by means of 43 pointing calibration observations, and the results pointed towards sub-arcsec accuracy; the change was made permanent in OD866. Subsequent checks pointed towards an APE† around 1.1 arcsec. (Table 4)

4.5 Pointing performance from OD1011 to the end of operations: full focal plane (FP) distortion correction

The full STR FP distortion correction (8 polynomial coefficients per axis) was computed by the FDS team at ESOC, based on the algorithm provided by the PACS ICC. In order to derive the final coefficients it was required to process raw data of guide stars for 20 consecutive ODs. This large volume of data was required to ensure that the parameter estimation was less sensitive to the non-calibratable biases in the measurements. Please refer to Section 2.3.1. of [27] for details on the procedures applied. This correction became operational in OD1011, producing a further improvement in the performance, APE$^{\dagger} \simeq 0.8$–0.9 arcsec.

In a third step (since OD1032), a number (73) stars from the STR catalogue that were deemed by the PACS ICC (see [5,10]) as "dubious" due to

positional uncertainties and/or high proper motions, affecting specific pointing directions, were removed from the tracking catalogue (the "tracking flag" was set to zero, and thus the stars can be used for acquisition but no longer for guiding), making the final figure ($APE^{\dagger} \simeq 0.8$–0.9 arcsec) rather homogeneous across the sky, assuming that a sufficient number of tracking stars are available. This value can be used as a proxy of the S/C absolute pointing accuracy during the last period of the mission operations' phase.. The pointing accuracy has nevertheless revealed quite sensitive to the SAA of the observations. Even moderately "warm" attitudes can produce an outstanding effect on the S/C pointing performance (see below).

4.6 Other pointing figures

4.6.1 Spatial relative pointing error (SRPE)

The relative pointing accuracy, as measured by the Spatial Relative Pointing Error (SRPE) has been only estimated for small raster maps (nodding observations with 52 arcsec throw). Nevertheless, even such a small size can yield representative SRPE results since the scale is larger than the usual STR bias stability range (~ 10 arcsec). Only two estimates have been done at present:

- At PVP, it was measured for non-interlaced (baseline conditions) and interlaced (goal conditions) observations, yielding an estimate of 1.54 arcsec (baseline)/1.1 arcsec (goal)
- In RSP, a further estimate was performed (M. Nielbock, PACS ICC) using 43 pointing calibration observations gathered in OD858 (i.e. when the STR1 2D correction was tested), yielding a result of 1.02 arcsec (mixed interlaced and non-interlaced observations).

4.6.2 Absolute pointing error in scan maps

The measurements of this figure have been performed using the PACS photometer in mini-map scan mode (two scan legs of 3 arcmin length, with 4 arcsec separation, at 70° and/or 110° tilt angle in instrument coordinates). Each scan direction was processed independently. The images were drizzled with a resolution of 0.1 pixel.

An early estimate was performed by means of 58 observations gathered between OD320 and OD762, so it is expected that the plate scale error effect has an impact on the results. Late measurements performed in cycles 64-71 (40 observations) confirmed that, after updating the on-board STR parameters with the full focal plane distortion correction, the Herschel scan map $APE^{\dagger}$ had substantially improved; therefore, a figure of $\simeq 0.9$ arcsec can be considered as reference for such observations in the last period of the mission. These figures are on the other hand almost identical to those obtained using the PACS photometer point source mode, as shown in Table 5.

Table 5 scan map APE†

Cycles	OD range	No. observations	$\langle \Delta Y \rangle$ (arcsec)	$\langle \Delta Z \rangle$ (arcsec)	σ_Y (arcsec)	σ_Z (arcsec)	APE† (arcsec)
30–33	595–650	58	0.38	0.77	1.24	2.01	2.36
64–71	1071–1182	40	0.61	0.76	0.52	0.74	0.90

4.6.3 Relative pointing error (RPE)

The relative pointing error (RPE) has been measured during PVP, both for fixed and moving targets. It meets or is better than the requirement of 0.3 arcsec: RPE = 0.19 arcsec for α Boo and RPE = 0.29 arcsec for the asteroid 19 Fortuna.

4.7 Solar System Objects' Tracking Performance

As stated in Section 1, the Herschel S/C was able to point and track Solar System Objects (SSO). These targets were uniquely defined by specifying their Navigation and Ancillary Information Facility (NAIF) ID[9] used to retrieve the information required to determine the coordinates at the observation time and also to calculate the differential tracking rate required. The ephemeris information was extracted from the NASA Jet Propulsion Laboratory (JPL) Horizons system[10]. The ephemeris file for a given object contained the geometric states with respect to the Solar System Barycentre (SSB), with a sampling period of 45 minutes. The SSO files were requested to be SSB-centric in order to perform the light-time and aberration correction in the correct frame via an iterative Newtonian approximation. A Hermite interpolating polynomial was used to obtain the ephemeris between the samples. The Herschel Scientific Mission Planning System computed the spacecraft-centric geometric state combining the Horizons ephemerides, the Herschel orbit file and JPL DE405 planetary and lunar ephemerides[11]. Finally, offsets were applied as required for the pointing pattern and the resulting quaternions were converted to ACA coordinates using the SIAM. The raster or line-scan pointings were performed relative to the SSO tracking frame. The tracking coefficients eventually uplinked to the S/C were defined as third-order Chebyshev polynomials describing the update quaternion as a function of time.

The SSO tracking performace was validated on two asteroids (a Jovian satellite was also foreseen, but eventually not executed) via PACS photometer observations executed during CoP and PVP [17,15]. The dedicated analysis of the 70 μm (blue) channel data (chop-nod and scan-map observations) showed perfect point sources with point-spread function (PSF) structures very similar

[9] `http://naif.jpl.nasa.gov/naif/about.html`
[10] `http://ssd.jpl.nasa.gov/horizons.cgi`
[11] `http://iau-comm4.jpl.nasa.gov/de405iom/de405iom.pdf`

to the ones obtained from fixed targets, demonstrating the high quality of the tracking performance and fulfilling all pre-launch requirements on tracking of moving targets. These results are consistent with the RPE measurements for moving targets performed in PVP and outlined in Section 4.6.3. The measurements taken in the context of testing the tracking performance (as part of the PACS focal plane geometry programme) are summarised in Table 6.

Table 6 Summary of measurements performed to test the SSO tracking performance.

OD	OBSID		Target	Duration	Filter	PACS photo mode	S/C-centric rate (arcsec/h)
41	1342179011	18	Melpomene	3304	blue/red	chop-nod	67.0
41	1342179012	18	Melpomene	2126	blue/red	scan-map	67.0
101	1342182740	8	Flora	4954	blue/red	chop-nod	51.3

In addition, tracked measurements on Mars, Neptune, Ceres, and Vesta have been used to characterise the PACS photometer PSF [16]

Around 800 moving targets (asteroids, comets, satellites, trans-Neptunian objects) with pre-calculated ephemeris information were available within the Herschel Observation Planning Tool (HSpot) and additional targets or ephemeris updates could be requested via Helpdesk tickets.

A few high-profile science targets required significantly faster tracking exceeding the nominal maximum speed (10 arcsec/min): 103P/Hartley 2 had an apparent Herschel-centric speed of 30 arcsec/min and 45P/Honda-Mrkos-Pajdusakova moved with about 36 arcsec/min during the Herschel observations. In both cases the differential tracking worked perfectly. There was only one near-Earth object which was too fast for Herschel's tracking capabilities: 2005 YU_{55} moved with 2.8-3.8 deg/hour (168-228 arcsec/min) and crossed the entire visibility window in about 16 hours. In this case, the observations were executed by scanning a fixed pre-calculated field on the sky while the target was crossing this field [18].

It is also worth noting the coordinate conventions in the final data products of tracked observations. The coordinates given in the final maps correspond to the Herschel-centric coordinates at the **start time** of the scientific measurement (the time connected to the first data frame taken; all subsequent data frames are then "stacked" onto this first frame), while the coordinates given in the product meta data are refering to the object's Herschel-centric coordinates at the **mid time** of the observation.

4.8 The impact of warm attitudes on the pointing accuracy

The first RSP measurements performed after OD1032 indicated an excellent behaviour of the pointing system, i.e. $APE^{\dagger} \simeq 0.85$ arcsec and 0.90 arcsec in point-source and mini-map modes, respectively. Nervetheless, a comprehensive

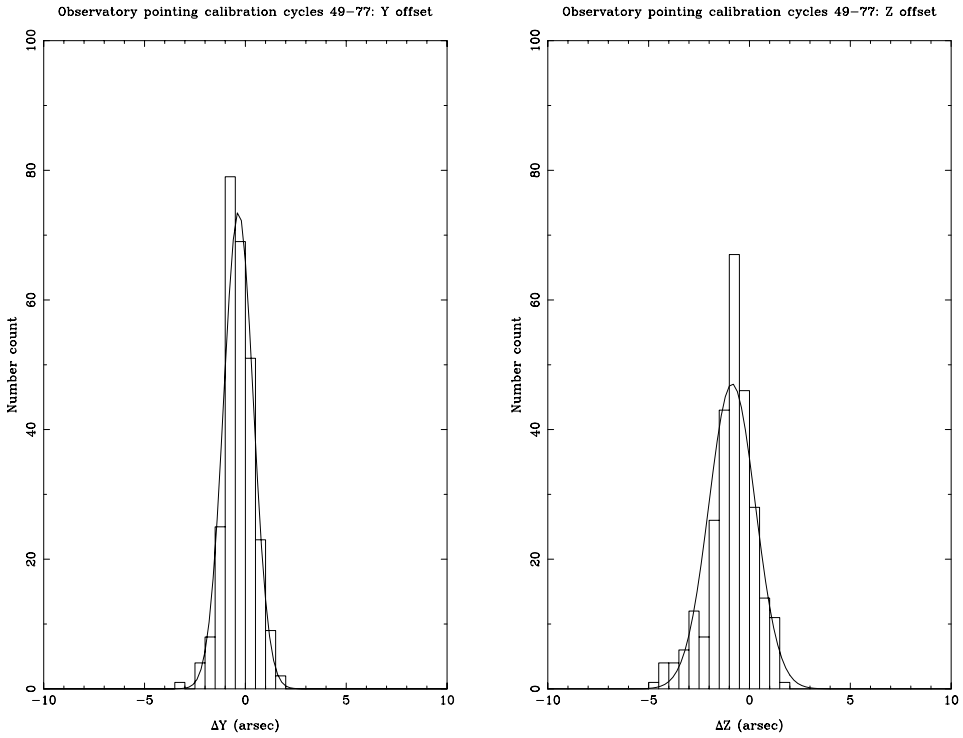

Fig. 4 Histograms of Y (left) and Z (right) pointing offset distributions. A clear asymmetry is observed towards the -Z direction

study compiling virtually all the pointing calibration observations gathered from the major STR focal plane update (OD866; see Section 4.4) revealed a distribution with rather large outliers, and with a clear asymmetry towards Z (see Fig. 4). Moreover, a relatively large offset was present in the average Y, Z position (see Table 7).

Table 7 APE† measurements, cycles 49 to 77

Cycles	OD range	No. observations	$\langle \Delta Y \rangle$ (arcsec)	$\langle \Delta Z \rangle$ (arcsec)	σ_Y (arcsec)	σ_Z (arcsec)	APE† (arcsec)
49–77	872–1266	271	-0.34	-0.86	0.73	1.15	1.36

This indicated that an additional factor was affecting the S/C pointing. A thorough study of the evolution of the attitude offsets across the whole period was performed (see Fig. 5): while the Y axis showed no trend (just

random dispersion around a zero offset), the Z axis exhibited a clear trend towards negative Z offsets, with two peaks separated by exactly one year. The offsets were apparently not associated to problems (e.g. incorrect astrometry) of the pointing targets themselves. Rather, the problem was traced to be related to the scheduling of long observations at negative beta (pitch) angles, corresponding to "warm" attitudes. As explained before, the term refers to attitudes where the STR supporting structures are subject to thermal distortions since they are not completely shaded from sunlight. In fact, in all but two cases of large astrometric Z offsets (larger than 2.5 arcsec), long periods (≥ 10 hr) at "warm" attitudes ($-20^\circ \leq \beta \leq -10^\circ$ i.e. $110^\circ \geq \mathrm{SAA} \geq 100^\circ$) took place two or less hours before the time of the pointing calibration observations. On the other hand, none of the correct (i.e. with reduced offset) observations investigated (randomly picked) were carried out in or after negative attitude periods. This indicated that the impact of relatively "mild" negative beta angles was larger than previously suspected. Therefore, scheduling restrictions in the range $110^\circ \geq \mathrm{SAA} \geq 100^\circ$ were enforced until the end of the operational mission.

After removing several suspicious ODs (872, 911, 932, 969, 1172, 1216, 1236, 1251, 1265 & 1266) from the statistics, the results improve, yielding a APE† estimate of ≈ 1.1 arcsec, better aligned with previous results. One of the challenges in the pointing area is the correct parametrisation of the pointing offset dependence on the SAA. This is a complex issue, since the pointing offset depends not only on the SAA of an observation, but also on the previous values of SAA. Moreover, the time scales of the pointing drift are not properly known.

One specially designed study for the pointing drift at extreme SAAs was conducted on OD 105 (August 26, 2009) within the PVP. The target HIP 117591 was observed at a SAA of 118.9 degrees. The S/C dwelled on this star for about 8.25 hours, and the centroids where monitored with the PACS photometer point-source mode observations at 70 μm. Immediately after this long staring observation (which was partitioned into three separate AORs of 2.75 hours, with their own initial target acquisition), short pointing observations were performed on a small list of stars with SAAs in the range [110,120] degrees. Finally, after around 12 hours total time of observations at these warm attitudes, the star HIP 72208 (being in the cold attitude with a SAA of 64.1 degrees) was acquired. A long staring observation for 8.25 hours, similar to the one for HIP 117591 was performed, to monitor the influence of the previous warm attitudes onto the pointing performance. We show the pointing results for the two long staring observations in Fig. 6. Note that for these graphs, the previously mentioned improvements regarding the STR distortions and the revision of the STR input catalogue were not applied. The starting point in the HIP 117591 drift plot thus reflects the typical result for the pointing performance of an individual object in this early phase of the mission. The relative offsets dy and dz in arcseconds from the expected centre position are shown. Since for both stars, the measurements are separated into three parts, each having 60 chop/nod cycles, each graph contains the information of 180 elementary pointing measurements. The time evolution is indicated by a colour

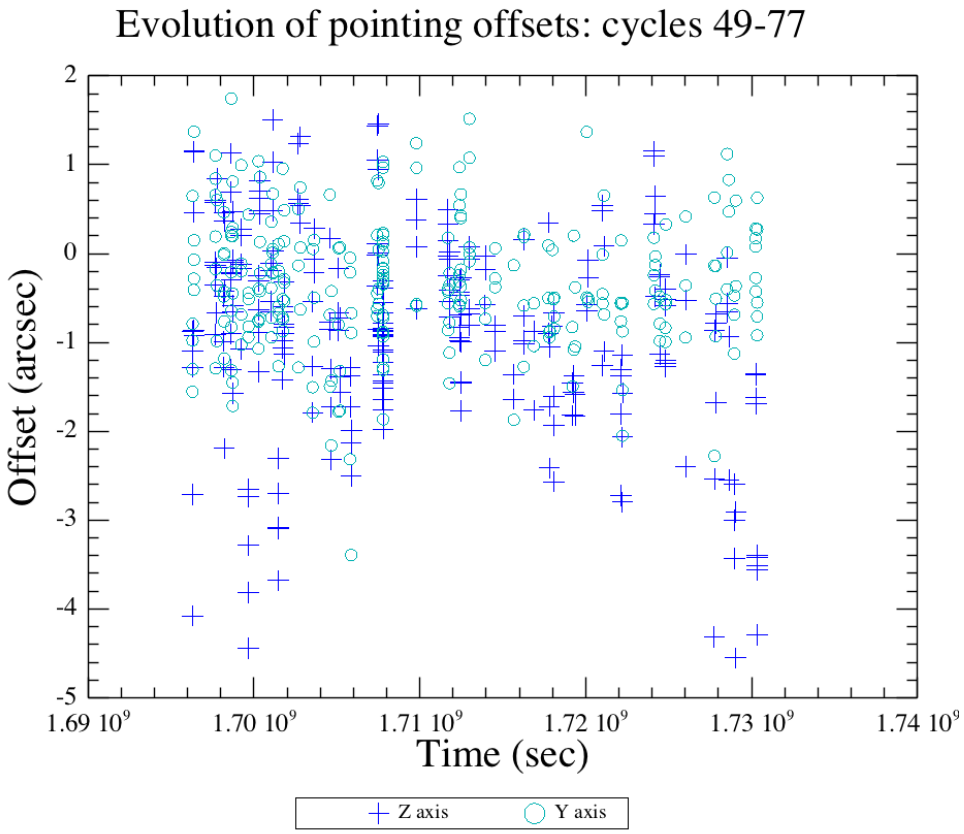

Fig. 5 Temporal evolution of the Y (circles) and Z (crosses) offsets from cycle 49 to 77 (OD872 to OD1266)

coding, going along the 8.25 hours per star from deep purple towards bright red. For HIP 117591, an evolution of the pointing offsets mainly in (negative) z-direction is clearly visible, an imprint of the warm attitude, which gets obvious after the first chunk of measurements, lasting for 2.75 hours. Also visible is the effect of re-pointing after 60 and 120 chop/nod cycles, which separates the offset values into three distinct clouds of points. The second graph, for HIP 72208, then demonstrates that after 12 hours at very warm attitudes, the relaxation to a normal pointing performance takes a long time. After the beginning of these observations at cold attitudes, the pointing offset in z-direction continues to increase further by roughly one arcsec, which might indicate a slight hysteresis effect in the thermal relaxation of the STR structures. Even after dwelling for 8.25 hours at this cold attitude, the pointing offset in z-direction did not improved much compared to the beginning of the measurement. This demonstrated that such extreme warm attitudes had to be avoided for normal S/C operations. It further showed that the temporal

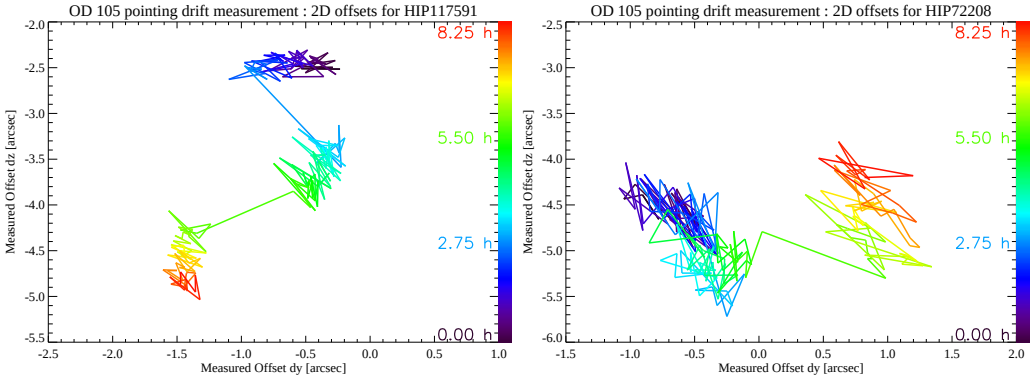
OD 105 pointing drift measurement : 2D offsets for HIP117591
OD 105 pointing drift measurement : 2D offsets for HIP72208
Measured Offset dz [arcsec]
Measured Offset dy [arcsec]
8.25 h
5.50 h
2.75 h
0.00 h

Fig. 6 Results of the pointing drift measurements from OD 105. Left: for star HIP 117591 (warm attitude). Right: for star HIP 72208 (cold attitude, after 12 hours of previous observations at warm attitude). The temporal evolution is indicated by the colour bar.

evolution of the pointing degradation, and an eventual relaxation to normal performance was a quite complex effect.

5 Improving the pointing performance

This section describes the efforts already implemented, currently on-going and future developments aimed towards optimising the *a posteriori* knowledge of the S/C pointing and therefore the accuracy of the astrometry in our products.

5.1 Implemented improvements

A simple offset correction software has been implemented at the HSC, applying the STR focal plane 2D linear correction (Section 2.4.1 of [27]) to each attitude within the pointing product. In summary, the software logic applies the steps below:

1. Load catalogue of stars from the STR, furnished by the ACMS manufacturers.
2. Open the pointing product and read its records in a loop. For each attitude sample:
   (a) Get the filtered attitude and the number of stars tracked (furnished in the STR quality flag field).
   (b) Get the catalogue information from those stars within the FoV of the STR at the current S/C filtered attitude[12]: X,Y,Z, magnitude, and trackability status.

[12] The STR is roughly pointing in the opposite direction to the telescope boresight.

(c) For the trackable stars within the FoV, determine the direction vectors using the STR "focal length" linear correction factors provided by FDS. These linear factors are introduced in the following way: the direction vector of a star in the STR boresight frame can be expressed in the small angle approximation as:

$$\mathbf{u_s} = \begin{pmatrix} 1 \\ -y/f \\ z/f \end{pmatrix} \sqrt{1 + (y/f)^2 + (z/f)^2} \tag{2}$$

Where y and z are the star's coordinates in the STR CCD frame, and f is the STR telescope's focal length. The linear "focal length" correction terms are introduced by replacing f by $f + \Delta f_y$ and $f + \Delta f_z$ in the Y and Z axes, respectively. Therefore, y/f gets replaced by $(y/f)(1 - (\Delta f_y/f) + O((\Delta f_y/f)^2))$ and an identical expression for the Z axis. Then, the corrected star vectors can be approximated as:

$$\mathbf{u'_s} \approx \begin{pmatrix} 1 \\ -\frac{y}{f}\left(1 - \frac{\Delta f_y}{f}\right) \\ \frac{z}{f}\left(1 - \frac{\Delta f_z}{f}\right) \end{pmatrix} \sqrt{1 + \left[\frac{y}{f}\left(1 - \frac{\Delta f_y}{f}\right)\right]^2 + \left[\frac{z}{f}\left(1 - \frac{\Delta f_z}{f}\right)\right]^2} \tag{3}$$

Specific correction factors have been derived and provided by FDS for the different mission periods up to OD866 (when the linear 2D was implemented on-board).

(d) Determine the tracked stars by means of the same selection algorithm used on-board the STR (limited to a maximum of nine stars)

(e) For the chosen stars, given the direction vectors and the inertial (reference) vectors, determine the best attitude using the ***q*** *Method* (see [28] and references therein) that provides a means for computing an optimal three-axis attitude from many vector observations.

(f) Replace the filtered quaternion by the modified quaternion computed by the ***q*** *Method*.

The applied correction does not add noise to the attitude samples since it is a purely geometric one. When the correction factors are set to 1.0, the input attitude is exactly recovered (within $\approx 1.0 \times 10^{-10}$ arcsec). In the current implementation, the software has some limitations, namely: *(i)* STR interlacing is not considered (a single STR "plane", using up to nine stars is processed). *(ii)* The stars' selection algorithm uses the same logic as the STR. But there is no check that the stars used within the script are the same as those actually used for tracking. In particular, if one of the 73 bad stars was used for tracking, it will be replaced by a different one by the correction software. *(iii)* The 2D linear correction is implemented, rather than the full one that includes eight polynomial terms per axis.

The simple reconstruction algorithm described above has been thoroughly tested in different scenarios. In particular, the full set of pointing calibration observations performed in cycles 23 to 41, comprising 245 observations

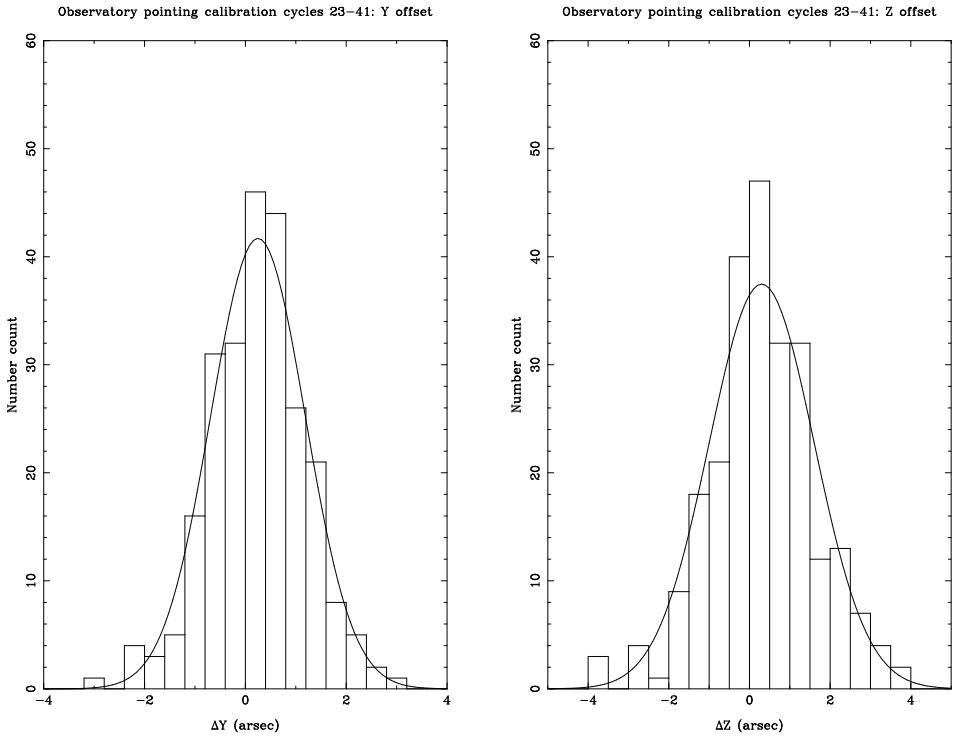

Fig. 7 Histograms of Y (left) and Z (right) pointing offset distributions obtained after applying the pointing reconstruction algorithm described in Section 5.1.

has been reprocessed using the improved pointing products. The results are shown in Fig. 7 and in Table 8. These results can be compared with those shown in Table 4. An outstanding example of the improvements achievable in some extreme cases is shown in Fig. 8. At the time of writing this paper, this correction has been applied to all observations in the Herschel Science Archive (HSA) from OD320 to OD865 (in OD866 the STR1 2D correction was applied and this ground correction is therefore not required) and a correction has been recently implemented for the first period of the mission (before OD320) and and will be applied to the observations in the HSA in the next bulk reprocessing. A summary of the accuracies achieved with the attitude data as given by the S/C and after ground processing is given in Table 10.

5.2 On-going developments and planned improvements

There are a number of on-going and planned developments to improve the *a posteriori* knowledge of the S/C pointing. A large effort has been done by the

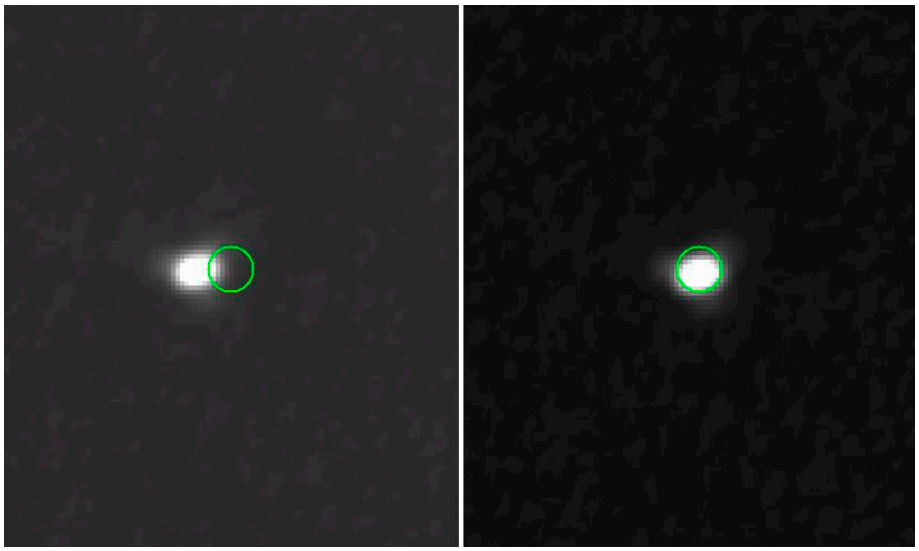

Fig. 8 A dramatic example of the effects of the simple pointing reconstruction described in Section 5.1: The PACS 70 μm map of the star UZ Tau was obtained in OD684. The observations towards the Taurus region show in general unusually large offsets due to the very asymmetric configuration of trackable stars in the STR boresight. The green circles are centred on the astrometric catalogue position of the target. The left panel shows the map with the original pointing product, while the right one presents the map processed with the reconstructed pointing product.The absolute astrometry offset is reduced from 7.5 arcsec to less than 1 arcsec.

Table 8 APE measurements using the reconstructed pointing products.

Cycles	OD range	No. observations	$\langle \Delta Y \rangle$ (arcsec)	$\langle \Delta Z \rangle$ (arcsec)	σ_Y (arcsec)	σ_Z (arcsec)	APE† (arcsec)
23–41	497–762	245	0.25	0.30	0.94	1.30	1.60

PACS ICC to improve the attitude measurements given by the STR, based not only on a full focal plane distortion correction but also taking into account the effects of the STR sub-pixel effects on the star centroiding caused by the pixel insensitive borders [11]. In addition, algorithms to propagate the attitude using the rate measurements given by the gyroscopes by means of the kinematic equation of motion (see for instance [28], p. 511) have been developed and benefit from the improved STR measurements (better estimates of the gyroscopes' drift rate biases and more accurate absolute pointing directions). Several studies have indicated that the pointing jitter may be accurately reconstructed using gyroscopes' measurements alone [3, 4, 12, 27].

In addition, several corrections affecting specific observations or ODs are being incorporated into the standard pipeline processing (SPG version 12.x and later). These include corrections for switch-over events from the prime to the redundant STR (these introduce offsets of some 15 arcsec), corrections

for resets of the S/C velocity vector (SVV) values used by the STR on-board software to compute the aberration correction of the coordinates of the guide stars (the lack of this correction can introduce offsets up to ≈ 20 arcsec) and *ad-hoc* corrections for pointing offsets (sometimes of several arcsec) induced by extreme "warm" attitudes.

Future developments being studied (to be implemented in the time frame 2014–2016) will likely include an attitude improvement software using batch least-squares estimators (these estimators update the state vector at a time using a block of observations taken during a fixed time span, as opposed to sequential estimators -e.g. Kalman filters- that update the state vector after each observation; see for instance [28], pp. 448-459) and a general modelling of the pointing offset induced by thermo-elastic distortions within the S/C.

6 Summary and conclusions

The Herschel's pointing system has experienced a complex evolution across the operational life of the S/C. Tables 9 and 10 summarise the sequence of main events and the evolution of the pointing accuracy accross the operational life of the observatory. The PVP demonstrated that the procedures devised within the calibration plan [17] were adequate to accomplish the mission of calibrating the alignment of a set of FIR and sub-mm instruments w.r.t. the S/C platform, without the help of ancillary optical instruments (e.g. the Quadrant Star Sensor on-board the Infrared Space Observatory –ISO; [14]). Moreover, the ACMS actual performance was found within the requirements and pre-flight predictions (only a non-compliance with the SRPE requirement was anticipated). Nevertheless, the reduction of the STR CCD reference temperature that was very successful to solve the "speed bumps" problem brought an unforeseen side-effect due to the plate scale changes within the STR. This new problem was hard to detect due to its dependence on the distribution of guide stars within the STR FoV, and highlights the importance of a continuous monitoring of the S/C pointing performance (preferentially with a wide sky coverage) to cope with changes in the ACMS behaviour. On the other hand, the pointing accuracy was found more sensitive than anticipated to attitudes where the STR supporting structures are subject to thermal distortions. This was also revealed thanks to large number of routine pointing calibration checks. In any case, it is worth stressing the fact that, even in the worst circumstances, the performance was within the requirements set (but for the SRPE as mentioned above). However, given a clear scientific motivation for further improvement an outstanding effort has been done and is still being invested in order to get the best from the attitude information. This collaborative effort is shared by different actors (at MOC, HSC, ICCs and industry) and reveals the high value of the communication and cooperation between different teams within the ground segment.

Table 9 Timeline of events

OD	Event	Effect
320	Lowering STR CCD reference temperature	"speed bumps" disappeared but STR plate scale errors suffered a considerable increment.
762	STR 1D correction	Improvement of the S/C-provided attitude information up to APE$^{\dagger} \approx 1.4$ arcsec
866	STR 2D correction	Further improvement of accuracy up to APE$^{\dagger} \approx 1.1$ arcsec
1011	STR full FP correction	Further improvement of accuracy up to APE$^{\dagger} \approx 0.9$ arcsec
1032	STR catalogue update (cleanup)	Improved accuracy in specific areas of the sky

Table 10 Summary of the evolution of the Herschel's astrometrical accuracy.

OD range	Raw accuracy APE† (arcsec)	Ground-processed APE† (arcsec)	Ground-correction available in SPG
32–320	1.9–2.2	1.4	> v11.1.0
321–761	2.4[a]	1.6	> v9.1.0
762–865	1.45	1.3	> v10.0.3
866–1010	1.1	–	N/A
1011–1452 (EoH)	0.9	–	N/A

[a] extreme outliers at ≥ 8 arcsec possible

Acknowledgements We acknowledge the anonymous referee for his/her valuable comments and suggestions. The Herschel spacecraft was designed, built, tested, and launched under a contract to ESA managed by the Herschel/Planck Project team by an industrial consortium under the overall responsibility of the prime contractor Thales Alenia Space (Cannes), and including Astrium (Friedrichshafen) responsible for the payload module and for system testing at spacecraft level, Thales Alenia Space (Turin) responsible for the service module, and Astrium (Toulouse) responsible for the telescope, with in excess of a hundred subcontractors.

PACS has been developed by a consortium of institutes led by MPE (Germany) and including UVIE (Austria); KU Leuven, CSL, IMEC (Belgium); CEA, LAM (France); MPIA (Germany); INAF-IFSI/OAA/OAP/OAT, LENS, SISSA (Italy); IAC (Spain). This development has been supported by the funding agencies BMVIT (Austria), ESA-PRODEX (Belgium), CEA/CNES (France), DLR (Germany), ASI/INAF (Italy), and CICYT/MCYT (Spain).

References

1. Herschel/Planck ACMS Users' Manual, H-P-4-DS-MA-001, (December 2006)
2. ASTR for Herschel/Planck User Manual, H-P-4-GAF-MA-0001, rev. 7 (October 2006)
3. Aussel, H., Towards an accurate reconstruction of the Herschel pointing. Technical Report SAp-PACS-HA-0729-11, issue 1.0, CEA Saclay (November 2011)
4. Aussel, H., PACS pointing jitter: the GYR view. Technical Report SAp-PACS-HA-0729-11, issue 1.0, CEA Saclay (November 2011)
5. Aussel, H., A first look into the STR catalog, CEA Saclay (27 July 2011)
6. Berrighi, G. and Lorenzini, S., Key Parameters for Herschel STR Catalogue Generation, Technical Note H-P-GAF-TN-0010, rev. 0 (4 February 2005)

7. De Grauuw Th. et al., The Herschel-Heterodyne Instrument for the Far-Infrared (HIFI), A&A, 518, L6 (2010)
8. Dungate, D.G., ESA Pointing Error Handbook, ESA-NCR-502 (Vol. 1), issue 1 (19 February 1993)
9. Elfving A., Rasmussen I., Herschel pointing accuracy and calibration procedures, SCI-PT-19552, rev. 1.3 (5 December 2003)
10. Feuchtgruber, H., Herschel Guide stars – Assessment of Quality, PICC-ME-TN-040, rev. 1.0 (8 December 2011)
11. Feuchtgruber, H., Herschel STR-A CCD Sub-Pixel Structure, PICC-ME-TN-041, rev. 2.0 (26 March 2012)
12. Feuchtgruber, H., Reconstruction of the Herschel Pointing Jitter, Technical Report PICC-ME-TN-042, rev. 1.0 (September 2012)
13. Griffin M.J. et al., The Herschel-SPIRE instrument and its in-flight performance, A&A, 518, L3 (2010)
14. Kessler M.F., Mller T.G., Leech K. et al., The ISO Handbook, Volume I: ISO – Mission & Satellite Overview, ESA SP-1262 (2003)
15. Klaas, U., et al., PACS Performance Verification Phase Plan, PICC-MA-PL-001, Issue 2.0. (2010)
16. Lutz, D., PACS photometer PSF, PICC-ME-TN-033, rev. 2.0 (4 April 2012) Available at `http://herschel.esac.esa.int/twiki/pub/Public/PacsCalibrationWeb/bolopsf_20.pdf`.
17. Marston, A. P., Sánchez-Portal, M. and the Herschel Pointing Working Group, Herschel Pointing Calibration Plan, HERSCHEL-HSC-DOC-1139, rev. 1.1 (2 April 2009)
18. Müller, T. et al. 2013, A&A, 558, 97
19. Nielbock, M. et al., PACS pointing calibration sources, PICC-MA-TN-003, rev. 1.1 (10 April 2008).
20. Nielbock, M., Müller, T., Klaas, U., et al., The Herschel PACS photometer calibration - A time dependent flux calibration for the PACS chopped point-source photometry AOT mode, Experimental Astronomy, 35 (2013)
21. Ott, S. 2010, ASP Conference Series, 434, 139
22. Pilbratt G.L. et al., Herschel Space Observatory, A&A, 518, L1 (2010)
23. Poglitsch A. et al., The Photodetector Array Camera and Spectrometer (PACS) on the Herschel Space Observatory, A&A, 518, L2 (2010)
24. Sánchez-Portal, M., Marston, A. P. and the Herschel Pointing Working Group, Herschel Routine Phase Pointing Calibration Plan, HERSCHEL-HSC-DOC-1622, rev. 0.1 (12 February 2010)
25. Sánchez-Portal, M., et al., Herschel Pointing Calibration Report, HERSCHEL-HSC-DOC-1515, rev. 1.0, (25 November 2009).
Available at `http://herschel.esac.esa.int/twiki/pub/Public/SpacecraftObservatoryWeb/pointing_calibration_report_v10.pdf`
26. Stephenson, C.A., Calculation of the 68th percentile of the Absolute Pointing Error, HERSCHEL-HSC-TN-2059, Issue 1.0 (December 2013)
27. Tuttlebee, M., Herschel/Planck Star Tracker Performance Assessment and Calibration, PT-CMOC-OPS-RP-6435-HSO-GF, Issue 1.0 (August 2013)
28. Wertz, J. R. (Ed.): Spacecraft Attitude Determination and Control, Kluwer Academic Publishers (1978)

Table 11 Contents of the pointing product (columns of each table data set/binary table)

Description	Name	Format	Unit	Comment
On-board time	obt	Double1d	μs	
Commanded pointing quaternion	commandQuat	Double2d	–	Contains the four double-precission components of the commanded attitude quaternion[a] in the ACA frame.
Filtered attitude quaternion	filterQuat	Double2d	–	Contains the four double-precission components of the filtered attitude quaternion in the ACA frame.[b]
Gyro-propagated attitude quaternion	gyroPropQuat	Double2d	–	Contains the four double-precission components of the gyro-propagated attitude quaternion in the ACA frame. If on-ground gyro-propagation is not enabled or available for the data record, this field contains a ground-derived filtered quaternion based on the nominal estimator.[c]
STR quality index	strQuality	Double1d	arcsec	Attitude quality index based on STR data. This quality index can be used as an error measurement for the filtered attitude.
Gyro-propagated quality index	gyroQuality	Double1d	arcsec	A quality index based on gyro propagation. If on-ground gyro-propagation is not enabled or available for the data record, this field contains a copy of the STR quality index.
S/C angular velocity	angVelocity	Double2d	arcsec/s	
S/C angular velocity error	angVelocityErr	Double2d	arcsec/s	
Constant velocity flag	isConstantVelocity	Bool1d	–	Relevant to scan maps. Set to 1 when the scan speed gets constant.
Quality flag	qualityFlag	Int1d	–	Its value corresponds to the number of tracked stars by the STR (the higher the number the better the quality of the derived attitude).
STR interlacing status	isInterlacing	Bool1d	–	1 if STR interlacing active, 0 otherwise.
Slew flag	isSlew (ISSLEW)	Bool1d	–	Set to 1 when the S/C is slewing.
On-target flag	isOnTarget	Bool1d	–	Set to 1 when the S/C is on-target.
Off-position flag	isOffPosition	Bool1d	–	Set to 1 when the S/C is at the attitude reference position (OFF position).
Out-of-field flag	isOutOfField	Bool1d	–	Set to 1 when the S/C is at the out-of-field referece attitude.
Uncorrected filtered attitude quaternion	uncorrFilterQuat	Double2d	–	Contains the four double-precission components of the STR-uncorrected filtered attitude quaternion in the ACA frame.[d]
Solar Aspect Angle	solarAspectAngle	Double1d	deg	Solar Aspect Angle (SAA) as provided in the AHF.

[a] The order of the components in any quaternion array is such as the scalar component goes in the last position.

[b] The "filtered" attitude refers to the attitude recomputed on-ground based on the available improvement algorithms, if available. Otherwise the column contains the same values as those stored in the "uncorrected filtered" attitude.

[c] The "gyro propagated" attitude refers to the attitude derived using the GYR outputs in telemetry to propagate an attitude quaternion derived from the on-board filtered attitude quaternion at an OFF-position prior to the execution of a raster or line scan.

[d] The "uncorrected filtered" attitude refers to the attitude computed by the ACMS combining STR and GYR outputs and down-linked in telemetry.